Electronic Ballasts Driven by Hybrid Source Using Microprocessor-Controlled Digital Switching Technique

Ying-Chun Chuang, Yu-Lung Ke
Department of Electrical Engineering
Kun Shan University
Tainan Hsien, Taiwan, R.O.C.
e-mail:chuang@mail.ksu.edu.tw
e-mail:yulungke@ms25.hinet.net

*Hung-Shiang Chuang, Mu-Lin Chou
*Department of Electrical Engineering
Kao Yuan University
Kaohsiung, Taiwan, R.O.C
e-mail:chuanghs@cc.kyu.edu.tw
e-mail:cady798@yahoo.com.tw

***Abstract*—A novel microprocessor-controlled electronic ballast with a class-E resonant inverter for illumination applications is employed to link a photovoltaic (PV)-powered battery energy storage system (BESS) as a main power source with a utility ac power as a complementary source. The proposed strategy aims to control power flow either from the PV-powered BESS or from the utility ac power line to the electronic ballast. This novel design has lower loss, easier control, and higher efficiency than the traditional photovoltaic panel has. A 27W fluorescent lamp is ignited by electronic ballast with a class-E topology to validate the proposed theoretical analyses. When the electronic ballast is driven by the PV-powered BESS and the utility ac power, overall efficiency of the proposed system is 94.2% and 91.1%, respectively. Experimental results demonstrate the functionality of the overall system, indicating that it is a good solution for several hybrid source applications.**

Keywords-electronic ballast; hybrid source; microprocerror; battery energy storage system; class-E resonant inverter.

I. INTRODUCTION

Giving growing public concern over the exhaustion of fossil fuel reserves and pollution problems incurred by conventional power generation, renewable energy sources such as solar, wind, micro-hydraulic, biomass, geothermal, hydrogen, and tidal are extensively adopted in industrial, commercial and military applications [1-6]. Moreover, fluctuations and increases in oil prices have negatively impacted the world economy, particularly economies in developing countries. Photovoltaic (PV) energy as an alternative energy source has been widely investigated as it is pollution-free, abundant and widely available. The PV energy applications can be divided into grid-connection systems and stand-alone systems. In grid-connection systems, an inverter stage plays an important role as the interface device between the PV power generation system and the utility. To connect to a utility, an inverter stage must be operated in grid-connection mode. Notably, an inverter stage can synchronize with utility ac sources. Additionally, inverters must be operated in switching mode when connected to a grid, and the current transferred onto a grid must be regulated to follow the reference signal. At the same time, active power switches of the inverter must be driven properly to generate a series of sinusoidal pulse width modulation (SPWM) waveforms. Then, through a LC low-pass filter, this inverter can generate sinusoidal voltage along with the utility to supply power to loads [7,8]. However, such PV systems are typically idle at night or during cloudy days. However, system components have not been used optimally. Conversely, traditional stand-alone systems have advantages of a simple system configuration and control scheme. To draw electrical power from PV arrays and store excess energy, a BESS is required. When output of a PV power generation system is insufficient, a BESS can provide backup energy; that is, a BESS works as an energy buffer. Furthermore, by using power electronic converters, stand-alone operation can be achieved easily and load-independent, high-quality voltage can be generated. Utilizing PV electricity to drive electronic ballasts may be one of the most appropriate applications of PV arrays with a BESS. Consequently, stand-alone systems have become the focus of research investigating PV-powered lighting applications.

The conventionally stand-alone PV-powered BESS for lighting applications has two power processing stages–an inverter stage and bridge rectifier stage. The inverter stage provides a low-frequency ac source of 50 or 60Hz, which is transferred to the downstream load, and the bridge rectifier stage generates a dc voltage for the electronic ballast which ignites a lamp and stabilizes lamp current during steady-state operation. However, the two-stage approach is costly, and reduces system reliability and efficiency, as energy is converted twice (Fig. 1). Moreover, this approach requires numerous components, thereby increasing final cost of the electronic lighting system and reducing system energy conversion efficiency.

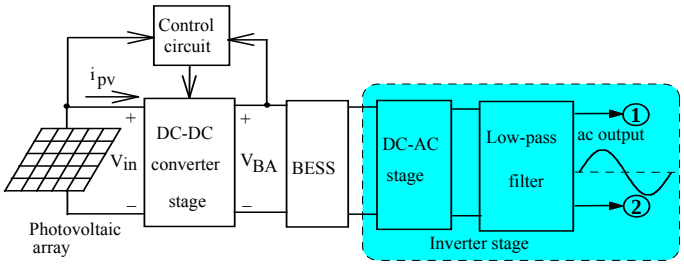

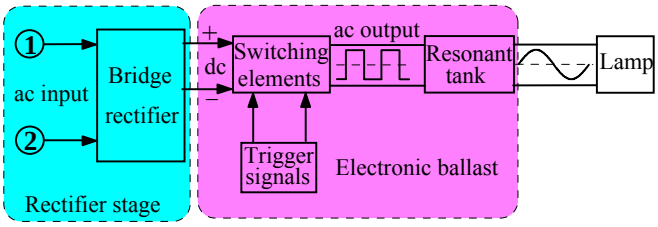

Fig. 1. Block diagram of a traditional PV-powered battery system for storing energy for lighting applications

These problems have promoted the use of high-frequency energy converters that convert dc electrical energy into energy for lighting. The simplest and least expensive method for converting PV power to dc electricity is to store energy in a BESS. The electronic ballast is directly connected to the BESS without an inverter stage or rectifier stage to improve conversion efficiency and decrease cost. Directly driven electronic ballast is then obtained that employs a PV-powered BESS (Fig. 2).

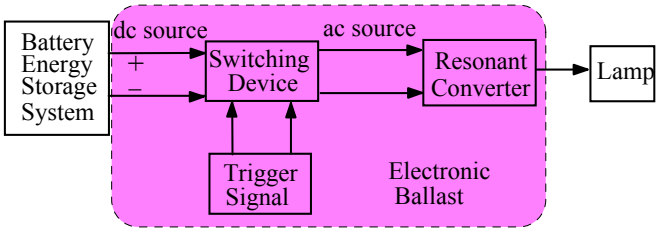

Fig. 2. Simplified block diagram of direct-driven electronic ballast by a PV-powered battery system for storing energy

Several lighting fixtures typically exist in lighting applications. Incandescent lamps and florescent lamps are the most common in lighting. Incandescent lamps and florescent lamps generate light via two physical mechanisms that convert electrical energy into light energy. Incandescent lamps exploit Joule-heating by electrically heating high-resistance tungsten filaments to an extreme brightness. The electrical behavior of incandescent lamps is simple. Lamp current is based on the applied voltage and the resistance of tungsten filament, whose *v-i* characteristic is close to that of a linear resistor. However, only about 10% of the electricity flowing through incandescent lamps is converted to light; thus, luminous efficiency of incandescent lamps is poor. Fluorescent lamps convert electrical energy into light by transforming electrical energy into the kinetic energy for moving electrons, which in turn produce radiation when they collide. Modifying the gas composition in fluorescent lamps can considerably alter luminous efficiency.

This study focuses on fluorescent lamps, which are utilized extensively in general lighting applications and have high luminous efficiency [9,10]. However, fluorescent lamps depend on a high striking voltage to generate and limit currents following ignition as they utilize negative incremental impedance. Thus, fluorescent lamps cannot be connected directly to a voltage source. Without limiting current, a lamp would be destroyed quickly, because of the negative resistance of fluorescent lamps. Consequently, some impedance must exist between a fluorescent lamp and the voltage source to limit lamp current. Most fluorescent lamps are operated using an ac source such that inductive impedance can be employed to limit current. AC operation also balances wear to the two electrodes and increase lamp life. Inductor ballasts are conventional ballasting, known as electromagnetic ballasts. Traditional electromagnetic ballasts are used to overcome these problems. Despite their low cost, ballasts cause bulbs to flicker are large, heavy and hum. Therefore, high-frequency electronic ballasts for fluorescent lamps have garnered considerable attention in recent years due to their light weight, small volume, high luminous efficiency and long lamp life. When a fluorescent lamp operates at a high frequency, luminous efficiency increases to about 20% higher than that achieved with conventional electromagnetic ballast operated at utility line frequency, thereby reducing the amount of energy consumed by the input power source.

Most high-frequency electronic ballasts have load resonant inverters that provide ignition voltage and a stable lamp current with a low crest factor for fluorescent lamps. Furthermore, load resonant inverters can operate at very high switching frequencies and have low switching losses and electromagnetic interference (EMI). To enhance the efficiency of high-frequency electronic ballasts, many soft-switching technologies have been developed [11-15]. The class-E zero-voltage-switching (ZVS) resonant inverters have the highest efficiency of all existing resonant inverters. The class-E ZVS resonant inverter has a single-ended structure and, thus, is unlike class-D ZVS inverters, which have a double-ended output and, thus requires two separate gate trigger signals and an upper trigger signal that has an isolated circuit. Additionally, the trigger circuit in the class-E topology, which has a single end, is simple. Consequently, the class-E ZVS resonant inverter has recently become common in switch-mode power applications. The use of a class-E ZVS resonant inverter as a fluorescent lamp ballast has such advantages as few components, low cost and high power density. These characteristics, combined with the fact that the class-E ZVS resonant inverter has only one active power switch, result in electronic ballast with a very simple structure, low switching losses, small volume and light weight. Additionally, as commutations in the active power switch of the class-E resonant inverter are performed at zero voltage, electronic ballast switching losses are extremely low, resulting in very high efficiency.

This work presents a novel application of electronic ballasts driven by a hybrid source [16,17]. In contrast to the conventional topology, the proposed configuration has no inverter stage for the main power source; rather it has a power-factor-correction (PFC) circuit and rectifier stage as the auxiliary power source. The PV arrays convert solar energy into dc electrical power, which can be used directly by electronic ballasts, where energy is stored in a BESS, and transformed to high-frequency ac power source using a high-frequency resonant inverter for fluorescent lamps. However, when a preset discharge threshold is attained, the load is disconnected from the BESS. A novel hybrid-source-powered

978-1-4244-3399-5/09/$25.00 Â© IEEE 2009

energy-saving lighting system is then employed for optimal use of the electronic ballast via microprocessor-controlled digital switching. Fig. 3 shows a typical configuration of proposed hybrid-source-powered lighting system with a digital switching feature. The proposed system is particularly suited to typically lighting applications. During daytime, this system effectively extract electrical power from PV arrays, while during nighttime, the system draws power from the utility for the lighting system with a high power factor (HPF) and high efficiency. The proposed system also requires a highly efficient illumination device such as a fluorescent lamp. To implement the two different energy control schemes and control the relay for switching operation modes, the proposed system has a microprocessor. Figure 4 shows a simplified block diagram of electronic ballast driven by using the microprocessor-controlled digital switching technique. In the proposed hybrid sources lighting system, circuit components must be designed carefully to reduce cost and improve reliability and efficiency. One benefit of the proposed topology of the electronic ballast is that it only requires one power processing stage, which makes it highly efficient, low-cost, reliable and simple. Hence, this study applies the power electronic load to a fluorescent lamp lighting system. The following sections present a detailed analysis and elucidate the function of the PV-powered electronic ballast.

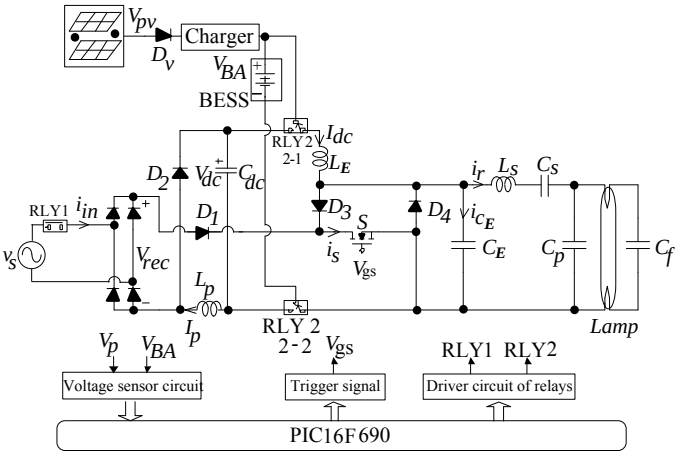

Fig. 3. Typical configuration of proposed hybrid-source-powered lighting system with a digital switching technique

The remainder of this paper is organized as follows. Section II describes the operating principle of electronic ballast with a class-E resonant inverter. Section III presents assumptions in analysis and the analytic results for the single-stage high-power-factor electronic ballast for fluorescent lamps. Section IV presents applications of the proposed electronic ballasts driven by a hybrid source using a microprocessor-controlled digital switching technique. The most important study results are also given in this section. Conclusions are presented in Section V.

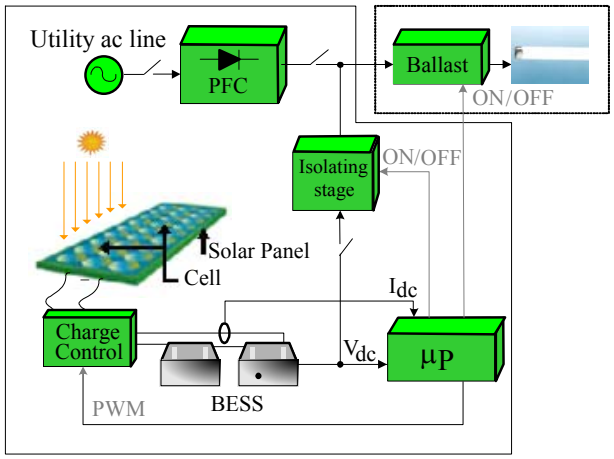

Fig. 4. Simplified block diagram of electronic ballast driven by using the microprocessor-controlled digital switching technique

II. Operating Principle of Electronic Ballat with Class-E Resonant Inverter

Unlike traditional ballast (Fig.1), this electronic ballast, which is driven by dc voltage, does not require an inverter stage with a large and heavy transformer with a filter circuit. Figure 5 schematically shows the circuit in the proposed single-switch electronic ballast for solar energy applications. The input terminal has a choke inductor L_E, which is generally large for the small ripple at the input dc current. The electronic ballast uses a class-E ZVS load resonant inverter to drive the fluorescent lamp. The diode D provides a path for the resonant current of the class-E ZVS resonant inverter. Metal–oxide–semiconductor field-effect transistors (MOSFETs) are preferred because their body diodes can be used as antiparallel diodes for operation beyond resonance. The fluorescent lamp is connected in parallel with a preheating capacitor C_f, which is in series with an resonant inductor L_S and a resonant capacitor C_S. The capacitor C_f provides a sufficiently high ignition voltage to the lamp during the initial start-up and then appropriate filament heating at a steady state. A resonant energy tanks, L_S, and C_S, which are in series with the lamp network, comprise the load resonant circuit of the class-E ZVS resonant inverter. The load resonant circuit of the class-E resonant inverter is formed by the fluorescent lamp and reactive components L_S, C_S C_p, and C_f In this investigation, the dc voltage V_{dc} is obtained from the BESS, which is fed by a PV array.

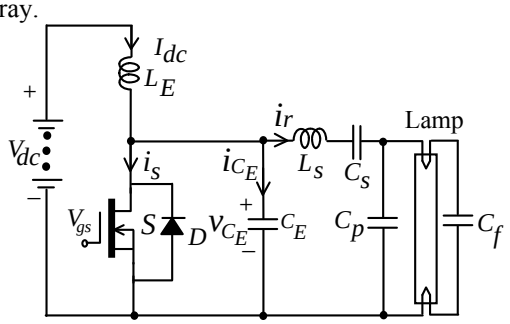

Fig. 5. Electronic ballast powered by a BESS

The electronic ballast with a class-E ZVS resonant inverter has an active power switch *S*, shunt capacitor C_E, an L_S-C_S-C_p resonant circuit, preheating capacitor C_f and fluorescent lamp. When operated at high frequency, the fluorescent lamp can be modeled as a resistance R_{lamp} and filament resistance r_f for each cathode. In practice, filament resistances of the fluorescent lamp are typically extremely small; therefore, they are not analyzed in this work. Then, the combination of C_p, C_f and the lamp (Fig. 5) connected in parallel is converted into a series combination of C_{ss} and R_{eq} (Fig. 5).

Equation (1) derives equivalent resistance R_{eq} and Eq. (2) derives equivalent capacitance C_{ss} (Fig.6).

$$R_{eq}=\frac{R_{lamp}}{1+\omega_s^2 R_{lamp}^2 (C_p+C_f)^2} \quad (1)$$

$$C_{ss}=\frac{C_s[1+\omega_s^2 R_{lamp}^2 (C_p+C_f)^2]}{1+\omega_s^2 R_{lamp}^2 (C_p+C_f)^2+\omega_s^2 R_{lamp}^2 C_s (C_p+C_f)} \quad (2)$$

Inductance L_E is assumed to be sufficiently large, such that the ac ripple on the dc-link current I_{dc} can be neglected.

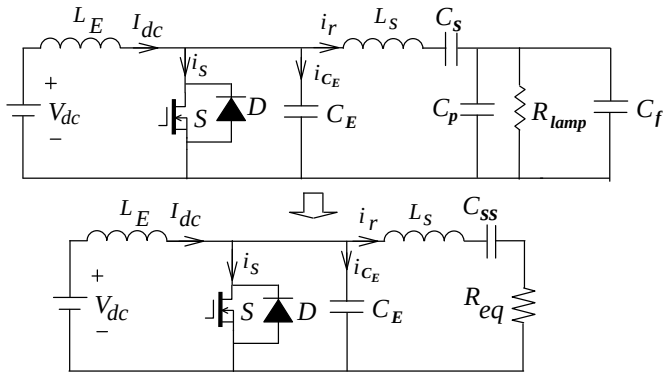

Fig. 6. Derivation of the equivalent circuit for the electronic ballast with the class-E resonant inverter

The PV-powered system is generally equipped with a BESS, which stores energy from a PV array during periods of high irradiation and provides electrical energy to the load during periods of low irradiation and at night. The charger circuit in the BESS is not analyzed. Since a BESS is a voltage source, using a voltage source converter simplifies system configuration. Figure 7 presents simplified schematics of a class-E ZVS resonant inverter. The following assumptions are used to elucidate the operation of a Class-E ZVS resonant inverter:

1) All circuit components are ideal.
2) The loaded quality factor of the class-E resonant inverter is sufficiently high, such that load current, i_r, is sinusoidal.
3) Inductance of the input inductor L_E is sufficiently high, such that input current is constant during each switching cycle.
4) The lamp is an open circuit before ignition, and a resistor in the steady state.

The driving signal V_{gs} first excites the active power switch of the proposed class-E electronic ballast. The duty cycle of the driving signal is *d*. Circuit operation can be divided into three modes based on the conducting power switch in a high-frequency cycle. Figure 8 displays the theoretical waveforms of the Class-E ZVS resonant inverter

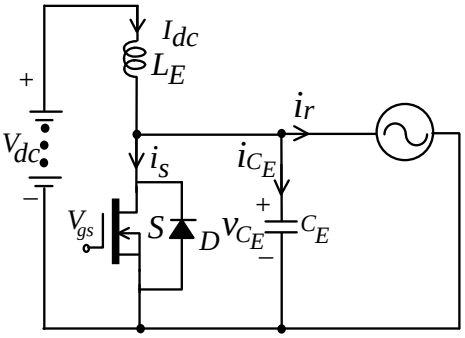

Fig. 7. Simplified equivalent circuit of the electronic ballast with the class-E ZVS resonant inverter

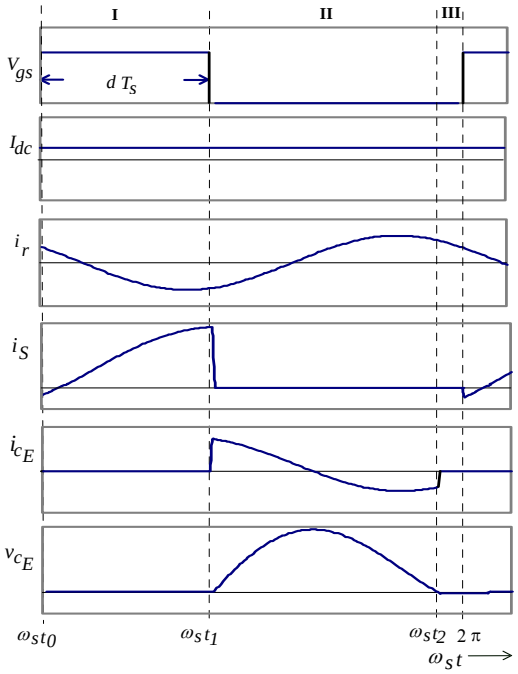

Fig. 8. Theoretical waveforms of the Class-E ZVS resonant inverter

Mode I ($\omega_S t_0 < \omega_S t < \omega_S t_1$):

Before $\omega_S t_0$, the active power switch, *S*, is off, and the freewheeling diode, *D*, is conducting. The current of diode *D* is the difference between inductor current I_{dc} and load resonant current i_r. At the start of this mode, a turn-on signal is sent to the gate of the switch *S*. Figure 9 shows the equivalent circuit in this mode. Once *S* is turned on, line voltage is transferred to the inductor L_E. In this analysis, the current i_r flowing into the load is assumed to be sinusoidal, and is described by Eq. (3),

where I_m is amplitude and ϕ is the initial phase angle of load current i_r.

$$i_r(t) = I_m \sin(\omega t + \phi) \tag{3}$$

The switch is closed and capacitance voltage, $v_{cE}(t)$, is 0, and current through the capacitor, $i_{cE}(t)$, is 0. Equation (4) derives the power switch current $i_S(t)$ in this time interval.

$$i_S(t) = I_{dc} - i_r(t) \tag{4}$$

The switch current, i_S, is comprised of source current and load current i_r. The active switch is turned off at zero voltage. When the active power switch, S, is off, its current is immediately diverted to the capacitor C_E.

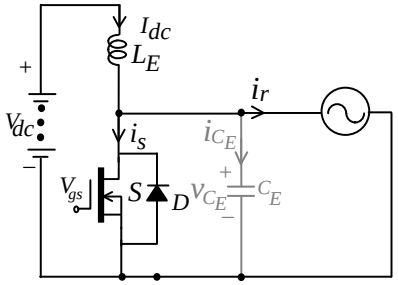

Fig. 9. Equivalent circuit of Mode I

Mode II ($\omega_S t_1 < \omega_S t < \omega_S t_2$):

In Mode II, the active power switch *S* is off. Figure 10 shows the equivalent circuit. The capacitor current $i_{cE}(t)$ is then the difference between I_{dc} and i_r. The voltage across the shunt capacitor is determined by Eq. (5).

$$v_c(t) = \frac{1}{\omega C_E}\left\{I_{dc}(\omega t - 2\pi d) + I_m\left[\cos(\omega t + \phi) - \cos(2\pi d + \phi)\right]\right\} \tag{5}$$

Substituting the condition of $i_{cE}(2\pi)=0$ into Eq. (5) yields the relationship among I_{dc}, I_m, d and ϕ.

$$I_m = I_{dc}\frac{2\pi(1-d)}{\cos(2\pi d + \phi) - \cos\phi} \tag{6}$$

The initial phase angle ϕ is acquired by substituting $i_s(2\pi)=0$ and Eq. (6) into Eq. (4).

$$\phi = \pi + \tan^{-1}\left[\frac{\cos(2\pi d) - 1}{2\pi(1-d) + \sin(2\pi d)}\right] \tag{7}$$

In steady-state operation, mean voltage is zero across the inductor. Mean capacitor voltage, v_{cE}, equals input voltage V_s.

$$V_S = \frac{1}{2\pi}\int_0^{2\pi} v_{cE}(\omega t)\,d(\omega t)$$

$$= \frac{I_{dc}}{\omega C_E}\left\{\frac{(1-d)\left[\pi(1-d)\cos(\pi d) + \sin(\pi d)\right]}{\tan(\pi d + \phi)\sin(\pi d)}\right\} \tag{8}$$

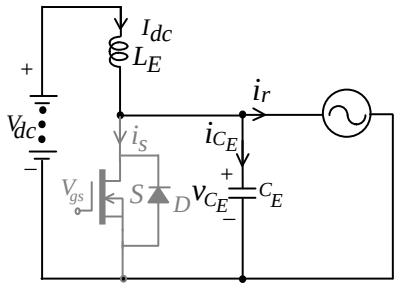

Fig. 10. Equivalent circuit of Mode II

Mode III ($\omega_S t_2 < \omega_S t < 2\pi$):

Mode III exists only when the switch voltage decreases to zero with a finite negative slope. The equivalent circuit of Mode III is similar to that of Mode I, except for initial conditions. The load resonant current falls to zero at the end of this mode. However, when circuit parameters are such that switch voltage decreases to zero with a zero slope, the diode D and this mode do not exist.

To ensure ZVS operation of the class-E resonant inverter, the circuit parameters must satisfy the following relationships [18]:

$$R_{eq} = \frac{2\sin^2(\pi d)\sin^2(\pi d + \phi)}{\pi^2(1-d)^2 P_{lamp}} V_s^2 \tag{9}$$

$$C_E = \frac{\sin(\pi d)\left[\sin 2(\pi d + \phi)\right]\left[(1-d)\pi\cos\pi d + \sin\pi d\right]}{\omega R_{eq}\pi^2(1-d)} \tag{10}$$

$$L_s = \frac{R_{eq}\left\{2(1-d)^2\pi^2 - 1 + 2\cos(\phi)\cos(2\pi d + \phi) - \cos 2(\pi d + \phi)\left[\cos(2\pi d) - \pi(1-d)\sin(2\pi d)\right]\right\}}{2\omega\sin(\pi d)\sin 2(\pi d + \phi)\left[(1-d)\pi\cos(\pi d) + \sin(\pi d)\right]} \tag{11}$$

III. Single-Stage High-Poweer-Factor Electronic Ballast for Fluorescent Lamps

Conventionally, when high-frequency electronic ballasts consume ac power from a utility, a diode-bridge rectifier with a bulk electrolytic capacitor is often utilized to convert ac voltage into smoothed dc-link voltage for high-frequency electronic ballasts. Such a rectifier circuit inevitably draws an input current with narrow pulses, which is notorious for having a very poor power factor and serious harmonic distortion. The power factor (PF) is typically ≤0.6 and total harmonic distortion (THD) can exceed 100%. The widespread use of high-frequency electronic ballasts for fluorescent lamps is a significant source of power pollution. However, a high power factor, including reductions in the rms line current and line current harmonic distortion, can cause a utility to increase its efficiency and reduce pollution. Therefore, high-frequency electronic ballast requires a filter circuit.

The most common solution for reducing input current harmonic distortion and improving the power factor of the utility ac source is to add a second power processing stage,

called the PFC stage. Such stages normally employ a discontinuous current dc-to-dc converter to make the line current follow the sinusoidal line voltage waveform. However, this two-stage approach increases cost, and reduces reliability and efficiency as power is processed twice. This problem can be solved by integrating the PFC circuit into the load resonant inverter stage. As a result of sharing the active power switch and control circuit, component count can be reduced. However, based on operation of the load resonant inverter stage, the active power switch must be switched at the desired frequency with the specified duty cycle. Under this constraint, the PFC circuit with a buck-boost topology is preferable as the high power factor for the PFC with a boost topology uses an excessively high dc-link voltage.

Figure 11 shows the circuit of the proposed single-stage high-power-factor electronic ballast. The electronic ballast comprises a class-E load resonant inverter for driving the fluorescent lamps and a buck-boost converter to shape input current. The buck-boost converter is formed by diodes $D_1$and D_2, inductor L_p, a dc-link capacitor C_{dc}, and active power switch S. The class-E resonant inverter has a dc-link capacitor C_{dc}, inductor L_E, diodes D_3 and D_4 and load resonant circuit. The diodes D_1 and D_3 are used for isolating the dc-link voltage and class-E resonant inverter. The diode D_4 provides a path for the resonant current of the class-E inverter. The fluorescent lamp is connected in parallel to a capacitor C_f, which is in series with an inductor L_S, and capacitor C_S. The capacitor C_f provides sufficiently high ignition voltage to the lamp during start-up, and then proper filament heating at a steady state. A resonant energy tank, L_S, and C_S, are linked in series to the lamp network, forming the load resonant circuit of the class-E resonant inverter. The load resonant circuit of the class-E inverter comprises the fluorescent lamps and reactive components L_S, C_S, C_p, and C_f.

Once the BESS has been discharged completely, the utility ac source is supplied to the single-stage high-power-factor electronic ballast (Fig.11). Operating the buck-boost converter at discontinuous conduction mode (DCM) reduces switching loss. Hence, the loss when the active power switch is switched on can be eliminated. Since the active power stitch S is turned on and off at a high fixed frequency with a constant duty cycle, the input current becomes a pulsating waveform at the same frequency. By properly controlling the pulsating current amplitude and duration, the average input current can be made sinusoidal and in phase with input voltage. The high-frequency harmonics of the input current is removed simply by using a small low-pass filter at the input terminal. Consequently, a near-unity power factor and very low harmonic distortion are attained.

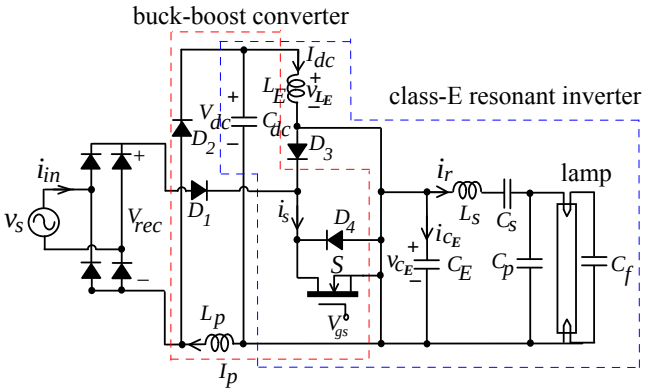

Fig. 11. Single-stage high-power-factor electronic ballast for a fluorescent lamp

The power for the buck-boost PFC stage is supplied by the utility ac source.

$$v_s(t) = V_m \sin(2\pi f_L t) \tag{12}$$

where V_m is amplitude of the ac line voltage source and f_L is line frequency.

When the active power switch S is on, the line source supplies current to the buck-boost stage. The unfiltered input current, i_{in}, equals I_p. Because the buck-boost PFC stage is operated at DCM over an entire line frequency cycle, I_p increases from zero at the instant when the active power switch, S, is turned on and peaks at the end of moment when the power switch S is turned on. Then, it decreases to zero before the end of moment when the active power switch is turned on. Figure 12 shows the current waveform of the inductor, L_p, in a completed utility line cycle. Its peak values follow a sinusoidal envelope and can be expressed as

$$I_{p,peak}(t) = d\frac{|V_m \sin(2\pi f_L t)|}{2L_p f_s} \tag{13}$$

where $|V_m \sin(2\pi f_L t)|$ is instantaneous line voltage, which can be considered constant for each switching cycle.

The average value of input current I_{in} within a high-frequency switching period can be calculated as

$$I_{in,ave}(t) = \frac{1}{T_s}\int_0^{T_s} I_p(t)d(t)$$

$$= \frac{d^2}{2L_p f_s} V_m \sin(2\pi f_L t) \tag{14}$$

Equation (14) indicates the input current is sinusoidal and in phase with the ac line voltage. Therefore, as the buck-boost PFC stage operates at DCM with a fixed switching frequency and constant duty cycle, the input current naturally follows the sinusoidal waveform of the utility ac line source.

Consequently, a high power factor of the utility ac line can be acquired.

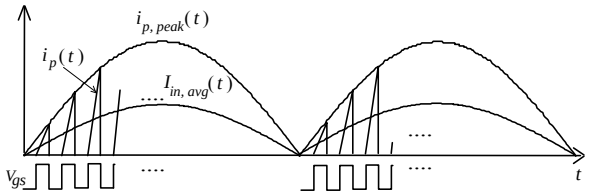

Fig. 12. Buck-boost inductor current waveformAbbreviations and Acronyms

IV. EXPERIMENT RESULTS

The proposed system (Fig.3) connects two different sources and two power relays. A programmable intelligent computer (PIC) microprocessor senses and controls the operation of peripheral interface devices such as the terminal voltage of the BESS, relay operational status, pulse-width-modulated (PWM) signal generation, and duty cycle control. Furthermore, the computer microprocessor controls energy management, including battery charging/discharging. The entire control system (Fig. 3) optimizes the energy performance of the hybrid system based on system state information, the BESS and the utility ac line. If the BESS operates at an output power condition (when providing energy to the electronic ballast, the terminal voltage of the BESS gradually declines), the microprocessor system only supervises the BESS policy of the hybrid source system. Once the terminal voltage of the BESS drops to the preset value, the utility ac line source supplies power to the single-stage high-power-factor electronic ballast. The microprocessor-controlled system controls energy management of the BESS energy system and output power of the utility ac line source system.

To verify the predicted operational principles and theoretical analysis of the proposed hybrid-source-powered lighting system with microprocessor-controlled digital switching technique, electronic ballast is designed and built to drive a 27W fluorescent lamp. The input voltage from the utility ac line is a sinusoidal wave of $110V_{rms}$ at 60Hz. To sustain a volt-second balance and avoid a spike current occurring at the instant of relay transition, the duty cycle of the active power switch must correspondingly adjust to accommodate the voltage across the BESS. The selected switching frequency for this prototype is set at 36.6 kHz. The single-stage high-power-factor electronic ballast operates with a duty cycle of 0.35 to generate a dc output voltage of 135V across a dc-link capacitor. Table 1 lists circuit parameters. Figure 13 shows the steady-state waveforms of the lamp voltage and lamp current of the electronic ballast, which is directly driven by the PV-powered BESS. The crest factor (CF) of the lamp current equals 1.43. Figure 14 shows the measured experimental waveforms of the experiment circuit, which are quite consistent with predicted results. Notably, the active power switch and the shunt capacitor C_E were also softly commutated under zero-voltage-switching conditions. Hence, the switching losses of this novel electronic ballast are near zero. Moreover, the experimentally obtained efficiency of the electronic ballast by the PV-powered BESS equals 94.21%. When the terminal voltage of BESS decreases to 105V, the relays are excited by the microprocessor and the utility ac line supplies power to the electronic ballast with a class-E topology. Therefore, single-stage high-power-factor electronic ballast is achieved. Figure 15 shows the transient response of lamp voltage and current waveforms of the electronic ballast during the switching period from the PV-powered BESS to the utility ac line. Transition time T_t=3.4ms is obtained. The results indicate that power transfer is very smooth and fast during the transfer period. The proposed ballast yields very good performance for lamp voltage and lamp current waveforms, which are similar to sinusoidal waveforms due to load characteristics of the class-E resonant inverter. Figure 16 shows the measured waveforms of the circuit components of the electronic ballast, which is driven by the utility ac line. Figure 17 shows the measured input line voltage and current waveforms when the PFC circuit is supplied by an input voltage of 110V. At this point in operation, the electronic ballast achieves a high power factor exceeding 0.998 and a low total harmonic distortion of $\leq$ 4.28%. The proposed system yields an efficiency of about 92.1% at the full load. This is about 2.1% lower than that when the electronic ballast is driven by a BESS as a rectifier stage and PFC. Figure 18 compares the requirements of international electrotechnical commission (IEC) 61000-3-2 Class C standard and measured input-current harmonics, which meets the IEC specifications.

Table 1 Circuit parameters

DC-link Capacitor C_{dc}	200μF
Inductor L_p	0.68mH
Inductor L_E	10mH
Inductor L_s	1.97mH
Capacitor C_E	9.35nF
Capacitor C_s	32.8nF
Capacitor C_p	6.5nF
Capacitor C_f	12nF

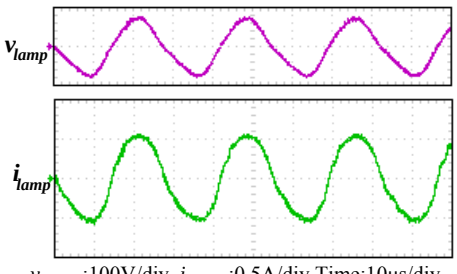

v_{lamp}:100V/div, i_{lamp}:0.5A/div,Time:10μs/div

Fig. 13. The measured waveforms of lamp voltage and lamp current

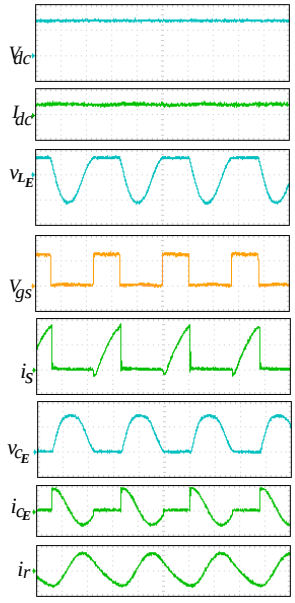

V_{dc}:100V/div, I_{dc}:0.5A/div, v_{L_E}:200V/div, V_{gs}:10V/div, i_S:0.5A/div, v_{C_E}:200V/div , i_{C_E}:1A/div, i_r:1A/div, Time:10μs/div

Fig. 14. The measured waveforms of the electronic ballast driven by the PV-powered BESS

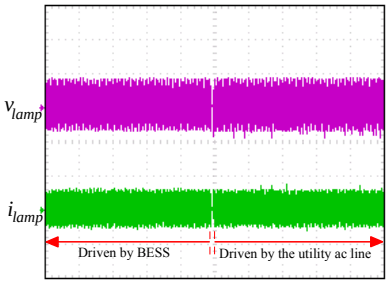

V_{lamp}:100V/div, I_{lamp}:1A /div, Time:50ms/div

Fig. 15. The lamp voltage and current waveforms of the electronic ballast operated at the transition period from BESS to the utility ac line.

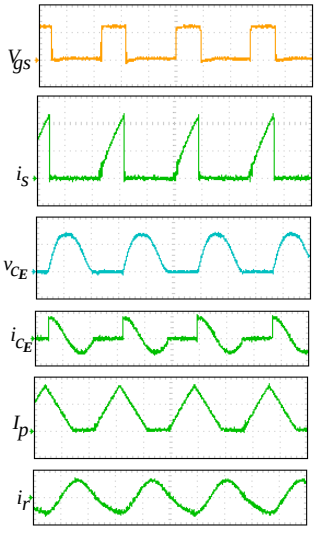

V_{gs}:10V/div, i_S:1A/div, v_{C_E}:200V/div , i_{C_E}:1A/div, I_p:1A/div, i_r:1A/div, Time:10μs/div

Fig. 16. Measured waveforms of the circuit components of the electronic ballast driven by the utility ac line

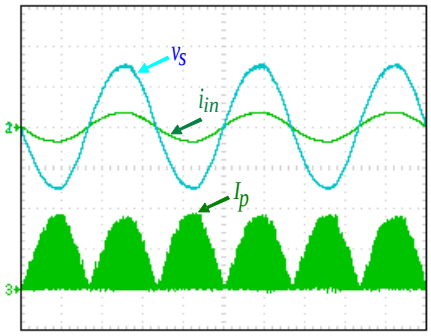

v_S:100V/div, i_{in}:1A/div, I_p:1A/div,Time:5ms/div

Fig. 17. Measured waveforms of v_S, i_{in}, *and* I_p

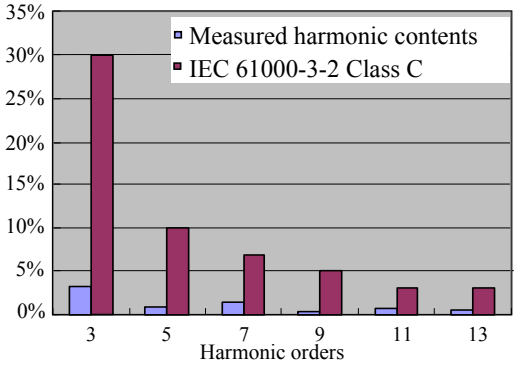

Fig. 18. Input current harmonic magnitude as percentage of the fundamental amplitude

V. CONCLUSIONS

This work presents novel electronic ballast with a simple structure, small volume, light weight, and low energy transfer losses. The electronic ballast circuit utilizes only a single active power switch and, unlike the traditional electronic ballast driven by a PV-powered BESS, does not require any output transformer. No power loss occurs between the BESS and electronic ballast without an additional power processing stage. Moreover, since commutations in the active power switch of the resonant inverter are achieved at zero voltage, electronic ballast switching losses are very low, resulting in extremely high efficiency. Consequently, ballast efficiency can be as high as 94.21%. A prototype of the proposed ballast for a 27W fluorescent lamp was implemented. As expected, a lamp current waveform with a low crest factor is obtained. The proposed topology is a viable solution for implementing low-cost high-efficiency electronic ballasts for PV-powered BESS applications.

Furthermore, when the voltage of the BESS declines to the preset discharge point, the microprocessor-controlled relays will automatically switch to the utility ac line that continuously supplies power for the electronic ballast. Under this operating condition, the single-stage structure is obtained by integrating a buck-boost converter for PFC and a class-E resonant inverter for the electronic ballast. Only one active power switch is commonly used by both power stages to reduce the cost of

active switches and control circuits. When the active power switch is softly switched at zero voltage and DCM, switching losses can be eliminated completely leading to high efficiency. Moreover, power losses are also be reduced by using few circuit components. Consequently, ballast efficiency is as high as 92.1%. Theoretical analysis and experimental results prove that a near-unity power factor and very low THD can be achieved. The proposed electronic ballast with microprocessor-controlled digital switching is a good solution for hybrid-source applications.

REFERENCES

[1] W. Wongsaichua, W. J. Lee, S. Oraintara, C. Kwan, F. Zhang, "Integrated High-Speed Intelligent Utility Tie Unit for Disbursed/Renewable Generation Facilities," IEEE Transactions on Industry Applications, Vol. 41, No. 2, March/April 2005, pp. 507-513.

[2] J. M. Carrasco, L. G. Franquelo, J. T. Bialasiewicz, E. Galvan, R. C. P. Guisado, Ma. A. M. Prats,J. I. Leon, N. Moreno-Alfonso, "Power-Electronic Systems for the Grid Integration of Renewable Energy Sources: A Survey" IEEE Transactions on Industrial Electronics, Vol. 53, No. 4, June 2006, pp. 1002-1016.

[3] A. Canova, L. Giaccone, F. Spertino,M. Tartaglia, "Electrical Impact of Photovoltaic Plant in Distributed Network," IEEE Transactions on Industry Applications, Vol. 45, No. 1, January/February 2009, pp. 341-347.

[4] C. Yang,K. M. Smedley, "One-Cycle-Controlled Three-Phase Grid-Connected Inverters and Their Parallel Operation," IEEE Transactions on Industry Applications, Vol. 44, No. 2, March/April 2008, pp. 663-671.

[5] S. Alepuz, S. Busquets-Monge, J. Bordonau, J. Gago, D. Gonzalez, J. Balcells, "Interfacing Renewable Energy Sources to the Utility Grid Using a Three-Level Inverter," IEEE Transactions on Industrial Electronics, Vol. 53, No. 5, October 2006, pp. 1504-1511.

[6] J. B.Cardell, and S. R. Connors, "Wind Power in New England: Modeling and Analysis of Nondispatchable Renewable Energy Technologies," IEEE Transactions on Power Systems, Vol. 13, No. 2, pp. 710-715, May 1998

[7] S. B. Kjaer, J. K. Pedersen, F. Blaabjerg, "A Review of Single-Phase Grid-Connected Inverters for Photovoltaic Modules," IEEE Transactions on Industry Applications, Vol. 41, No. 5, September/October 2005, pp. 1292-1306.

[8] C. A. Hernandez-Aramburo, T. C. Green, N. Mugniot, "Fuel consumption minimization of a microgrid," IEEE Transactions on Industry Applications, Vol. 41, No. 3, May/June 2005, pp. 673-681.

[9] S. Ben-Yaakov, M. Shvartsas, S. Glozman, "Statics and Dynamics of Fluorescent Lamps Operating at High Frequency: Modeling and Simulation," IEEE Transactions on Industry Applications, Vol. 38, No. 6, November/December 2002, pp. 1486-1492.

[10] S. Glozman, S. Ben-Yaakov, S, "Dynamic Interaction Analysis of HF Ballasts and Fluorescent Lamps Based on Envelope Simulation," IEEE Transactions on Industry Applications, Vol. 37, No. 5, September/October 2001, pp. 1531-1536.

[11] F. J. F. Martin, C. B. Viejo, J. C. A. Anton, M. A. P. Gacia, M. Rico-Secades, and J. M. Alonso, "Analysis and Design of a High Power Factor, Single-Stage Electronic Ballast for High-Intensity Discharge Lamps," IEEE Transactions on Power Electronics, Vol. 18, No. 2, March 2003, pp. 558-569.

[12] M. Brumatti, M. A. Co, D. S. L. Simonetti and J. L. F. Jose, " Single Stage Self-Oscillating HPF Electronic Ballast," IEEE Transactions on Industry Applications, Vol. 41, No. 3, May/June 2005, pp. 558-569.

[13] K. Jirasereeamornkul, M. K. Kazimierczuk, I. Boonyaroonate, and K. Chamnongthai, " Single-Stage Electronic Ballast with Class-E Rectifier as Power-Factor Corrector," IEEE Transactions on Circuits and Systems-I: Regular Papers, Vol. 53, No. 1, January 2006, pp. 139-148.

[14] Y. C. Chuang, and H. L. Cheng, "Single-Stage Single-Switch High-Power-Factor Electronic Ballast for Fluorescent Lamps," IEEE Transactions on Industry Applications, Vol. 43, No. 6, November/December 2007, pp. 1434-1440.

[15] Y. C. Chuang, Chin-Sien Moo, Hsien-Wen Chen, and Tsai-Fu Lin, "A Novel Single-Stage High-Power-Factor Electronic Ballast with Boost Topology for Multiple Fluorescent Lamps," IEEE Transactions on Industry Applications, Vol. 45, No. 1, January/February 2009, pp. 323-331.

[16] O. Briat, J. M. Vinassa,W. Lajnef, S. Azzopardi, E. Woirgard, "Principle, Design and Experimental Validation of a Flywheel-Battery Hybrid Source for Heavy-Duty Electric Vehicles," IET Electric Power Applications, Vol. 1, No. 5, September 2007, pp. 665-674.

[17] A. Barrado, R. Vazquez, E. Olias, A. Lazaro,J. Pleite, "Theoretical Study and Implementation of a Fast Transient Response Hybrid Power Supply," IEEE Transactions on Power Electronics, Vol. 19, No. 4, July 2004, pp. 1003-1009.

[18] M. K. Kazimierczuk and D. Czarkowski, "Resonant Power Converters," Wiley, New York, 1995.

978-1-4244-3399-5/09/$25.00 Â© IEEE 2009